PTEP

Prog. Theor. Exp. Phys. **2019**, 043B03 (19 pages)
DOI: 10.1093/ptep/ptz022

Construction of a renormalization group improved effective potential in a two real scalar system

Hideaki Okane*

Graduate School of Science, Hiroshima University, Higashi-Hiroshima 739-8526, Japan
*E-mail: hideaki-ookane@hiroshima-u.ac.jp

Received January 20, 2019; Revised February 21, 2019; Accepted February 26, 2019; Published April 16, 2019

We study the improvement of an effective potential by a renormalization group (RG) equation in a two real scalar system. We clarify the logarithmic structure of the effective potential in this model. Based on the analysis of the logarithmic structure of it, we find that the RG improved effective potential up to Lth-to-leading log order can be calculated by the L-loop effective potential and $(L+1)$-loop β and γ functions. To obtain the RG improved effective potential, we choose the mass eigenvalue as a renormalization scale. If another logarithm at the renormalization scale is large, we decouple the heavy particle from the RG equation and we must modify the RG improved effective potential. In this paper we treat such a situation and evaluate the RG improved effective potential. Although this method was previously developed in a single scalar case, we implement the method in a two real scalar system. The feature of this method is that the choice of renormalization scale does not change even in a calculation of higher leading log order. Following our method one can derive the RG improved effective potential in a multiple scalar model.

Subject Index B32, B36

1. Introduction

Effective potentials improved by a renormalization group (RG) equation are widely applied in particle physics. In Refs. [1–6], the stability of an electroweak vacuum is studied through the evaluation of the RG improved effective potential on the high-energy scale. In addition, using the RG improved effective potential, the authors of Refs. [7–18] investigate the possibility that spontaneous symmetry breaking is realized by quantum correction to the effective potential. In this way, the RG improved effective potential is frequently utilized.

There has been a great deal of research into the RG improvement of the effective potential since a study by Coleman and Weinberg [7]. In Refs. [19–21], the RG improved effective potential in a single field is derived. If utilizing the RG invariance of the effective potential, the renormalization scale μ is set as a field-dependent mass $M(\phi,\mu)$; the logarithm $\log(M(\phi,\mu)^2/\mu^2)$ becomes zero. In that case, the logarithmic perturbative expansion of the effective potential including $(\log(M(\phi,\mu)^2/\mu^2))^L$ at the L-loop level is stable because of $\log(M(\phi,\mu)^2/\mu^2) = 0$. This is an essential point for the construction of the RG improved effective potential. If the theory includes multiple fields, the situation is not so simple. Taking $M(\phi,\mu)$ as a renormalization scale, one cannot guarantee that the logarithm $\log(M'(\phi,\mu)^2/\mu^2)$ coming from another field is always small. If the logarithm is large,

Funded by SCOAP[3]

it leads to the breakdown of the perturbative expansion for the effective potential. In Refs. [22–26], the methods of solving such a problem are studied. The methods are classified into two types. In Refs. [22–24], multiple renormalization scales are introduced and each logarithm is suppressed by the multiple renormalization scales. On the other hand, the decoupling theorem [27] is applied in Refs. [25,26]. If a large logarithm appears in the calculation of the effective potential, the heavy particle is decoupled. Since the remaining logarithm is only one of a light field, the calculation of the RG improved effective potential is the same as the method explained in the single field case. Note that these methods are applied to theory including only a single scalar field.

If multiple scalar fields are introduced, the analysis of the RG improved effective potential is complicated because the masses appearing in the logarithms depend on multiple classical background fields such as $M(\phi_1, \phi_2)$. The problem is addressed in Refs. [28–30]. In Ref. [28], the RG improved effective potential is calculated with the introduction of the multiple renormalization scale. In Ref. [29], which extends the method of Ref. [26], a step function for the automatic decoupling of a heavy particle is introduced in the effective potential. Moreover, effective action is analyzed to take wavefunction renormalization into account. In Ref. [30], a new method is suggested. The guiding principle for the method is to choose the renormalization scale so that the total loop correction vanishes. In Ref. [31] the RG improved effective potential in classical conformal theory is analyzed based on the method of Ref. [30]. In the present paper, we also approach the problem for the RG improvement of the effective potential.

In this paper, extending the method of Ref. [25], we construct the RG improved effective potential in a two real scalar theory. Since the method of Ref. [25] is based on the analysis of the logarithmic structure of the effective potential, we derive the expression of the effective potential expanded with respect to all the logarithms appearing in a two real scalar system. Based on the analysis of the logarithmic structure of the effective potential, we choose the field-dependent mass eigenvalue as a renormalization scale so that one of the logarithms vanishes. If another logarithm at the renormalization scale is small enough to be perturbative, the RG improved effective potential is calculated with the choice of the renormalization scale. If the logarithm is large, we absorb the logarithm into the new parameters defined in the low-energy scale and decouple the heavy particle from the theory. Since the logarithm to be considered is only one of a light particle, we can easily evaluate the RG improved effective potential. The advantages of this method are as follows. First, since this method is based on the logarithmic structure of the effective potential at any loop order, the choice of the renormalization scale does not need to be changed even at higher loop order. Second, we can derive the RG improved effective potential without introducing multiple renormalization scales or a step function for the decoupling. Finally, we can easily implement the decoupling theorem by expanding the effective potential coming from quantum correction with respect to ϕ^2/m^2 ($\phi^2 = \phi_1^2 + \phi_2^2$, m: decoupling scale).

This paper is organized as follows: In Sect. 2, we clarify the logarithmic structure of the effective potential and investigate the choice of the renormalization scale. In Sect. 3, the massless theory is treated and the RG improved effective potential is calculated based on the analysis of Sect. 2. In Sect. 4, we consider the massive model. In this section, we face a situation in which a large logarithm occurs. We decouple the heavy particle and construct the RG improved effective potential on the low-energy scale. In Sect. 5, we summarize the procedure of RG improvement in a multiple scalar model and discuss applications to other models. In Appendix A, the β and γ functions at the 1-loop level are given.

2. Logarithmic structure of effective potential and RG improvement

In this section, we clarify the logarithmic structure of the effective potential based on Ref. [25]. We then consider the choice of renormalization scale for the RG improvement of the effective potential. For a more specific explanation, we consider a two real scalar system as an example. The Lagrangian is given as follows:

$$\mathcal{L} = \frac{1}{2}(\partial\sigma)^2 + \frac{1}{2}(\partial\chi)^2 - \frac{m_1^2}{2}\sigma^2 - \frac{m_2^2}{2}\chi^2 - \frac{\lambda_1}{4!}\sigma^4 - \frac{\lambda_2}{4!}\chi^4 - \frac{\lambda_3}{4}\sigma^2\chi^2 - \Lambda. \tag{1}$$

We suppose that this model has $Z_2 \times Z_2$ symmetry: $\sigma \to -\sigma$ and $\chi \to -\chi$. Following Ref. [25], we factor out a coupling constant $1/\lambda_1$ from the Lagrangian[1]

$$\begin{aligned}\mathcal{L} = \frac{1}{\lambda_1}\Bigg(&\frac{1}{2}\left\{\partial(\sqrt{\lambda_1}\sigma)\right\}^2 + \frac{1}{2}\left\{\partial(\sqrt{\lambda_1}\chi)\right\}^2 - \frac{m_1^2}{2}(\sqrt{\lambda_1}\sigma)^2 - \frac{m_2^2}{2}(\sqrt{\lambda_1}\chi)^2 \\ &- \frac{1}{4!}(\sqrt{\lambda_1}\sigma)^4 - \frac{\lambda_2/\lambda_1}{4!}(\sqrt{\lambda_1}\chi)^4 - \frac{\lambda_3/\lambda_1}{4}(\sqrt{\lambda_1}\sigma)^2(\sqrt{\lambda_1}\chi)^2 - \lambda_1\Lambda\Bigg).\end{aligned} \tag{2}$$

Next, we shift the fields (σ, χ) by classical background fields (ϕ_1, ϕ_2), respectively:

$$\sigma \to \phi_1 + \sigma,$$
$$\chi \to \phi_2 + \chi,$$

and then redefine the quantum fields $\sqrt{\lambda_1}\sigma$ and $\sqrt{\lambda_1}\chi$ as σ and χ, respectively. After the shift and the redefinition, the Lagrangian becomes

$$\begin{aligned}\mathcal{L} = \frac{1}{\lambda_1}\Bigg(&\frac{1}{2}(\partial\sigma)^2 + \frac{1}{2}(\partial\chi)^2 - \frac{M_1^2}{2}\sigma^2 - \frac{M_2^2}{2}\chi^2 - M_3^2\sigma\chi \\ &- \frac{x_1}{3!}\sigma^3 - \frac{x_2 y_1}{3!}\chi^3 - \frac{y_2}{2}(x_2\sigma + x_1\chi)\sigma\chi \\ &- \frac{1}{4!}\sigma^4 - \frac{y_1}{4!}\chi^4 - \frac{y_2}{4}\sigma^2\chi^2 - \lambda_1 V^{(0)}\Bigg),\end{aligned} \tag{3}$$

where mass parameters (M_1^2, M_2^2, M_3^2), cubic coupling constants (x_1, x_2), and quartic coupling constants (y_1, y_2) are introduced as follows:

$$\begin{aligned} M_1^2 &= m_1^2 + \frac{\lambda_1}{2}\phi_1^2 + \frac{\lambda_3}{2}\phi_2^2, \\ M_2^2 &= m_2^2 + \frac{\lambda_3}{2}\phi_1^2 + \frac{\lambda_2}{2}\phi_2^2, \\ M_3^2 &= \lambda_3\phi_1\phi_2, \\ x_1 &= \sqrt{\lambda_1}\phi_1, \qquad x_2 = \sqrt{\lambda_1}\phi_2, \\ y_1 &= \frac{\lambda_2}{\lambda_1}, \qquad y_2 = \frac{\lambda_3}{\lambda_1}, \end{aligned}$$

[1] In this paper, we assume that all the quartic coupling constants are comparable to each other ($\mathcal{O}(\lambda_1) \sim \mathcal{O}(\lambda_2) \sim \mathcal{O}(\lambda_3)$) and perturbative. Under this assumption, the choice of λ_1 does not affect the final expression (28). That is to say, factoring out λ_2 (or λ_3) replaced by λ_1, one obtains the same result (28).

and $V^{(0)}$ is a tree-level effective potential:

$$V^{(0)} = \frac{m_1^2}{2}\phi_1^2 + \frac{m_2^2}{2}\phi_2^2 + \frac{\lambda_1}{4!}\phi_1^4 + \frac{\lambda_2}{4!}\phi_2^4 + \frac{\lambda_3}{4}\phi_1^2\phi_2^2 + \Lambda. \tag{4}$$

From the rewritten Lagrangian (3) and the tree potential (4), we can find that the theory is described by the following parameters:

$$\text{mass parameters :} \quad M_1^2,\ M_2^2,\ M_3^2, \tag{5}$$

$$\text{cubic coupling constants :} \quad x_1,\ x_2, \tag{6}$$

$$\text{quartic coupling constants :} \quad \lambda_1,\ y_1,\ y_2, \tag{7}$$

$$\text{constant term :} \quad \Lambda. \tag{8}$$

Moreover, since it is inconvenient for the mass matrix not to be diagonal, we rotate the mass matrix by introducing new states (σ_d and χ_d) and mixing angle (θ):

$$\begin{pmatrix}\sigma\\ \chi\end{pmatrix} = \begin{pmatrix}\cos\theta & -\sin\theta\\ \sin\theta & \cos\theta\end{pmatrix}\begin{pmatrix}\sigma_d\\ \chi_d\end{pmatrix}, \quad \tan(2\theta) = \frac{2M_3^2}{M_1^2 - M_2^2},$$

and then the mass matrix is diagonalized:

$$\begin{pmatrix}\sigma & \chi\end{pmatrix}\begin{pmatrix}M_1^2 & M_3^2\\ M_3^2 & M_2^2\end{pmatrix}\begin{pmatrix}\sigma\\ \chi\end{pmatrix} = \begin{pmatrix}\sigma_d & \chi_d\end{pmatrix}\begin{pmatrix}M_+^2 & 0\\ 0 & M_-^2\end{pmatrix}\begin{pmatrix}\sigma_d\\ \chi_d\end{pmatrix},$$

where the mass eigenvalues are

$$M_\pm^2 = \frac{1}{2}\left(M_1^2 + M_2^2 \pm \sqrt{(M_1^2 - M_2^2)^2 + 4M_3^4}\right).$$

For later discussion, the coordinate (ϕ_1, ϕ_2) is translated to the polar coordinate (ϕ, β):

$$\phi^2 = \phi_1^2 + \phi_2^2, \qquad \tan\beta = \frac{\phi_2}{\phi_1}. \tag{9}$$

From now on, the mass eigenvalues and the effective potential are written with the polar coordinate (ϕ, β).

At this stage, we can replace the three mass parameters (M_1^2, M_2^2, M_3^2) in Eq. (5) by mass eigenvalues $(M_\pm^2)$ and mixing angle (θ). Namely, the model is described in terms of the following parameters:

$$\text{mass eigenvalues :} \quad M_\pm^2, \tag{10}$$

$$\text{mixing angle :} \quad \theta, \tag{11}$$

$$\text{cubic coupling constants :} \quad x_1,\ x_2, \tag{12}$$

$$\text{quartic coupling constants :} \quad \lambda_1,\ y_1,\ y_2, \tag{13}$$

$$\text{constant term :} \quad \Lambda. \tag{14}$$

This information is so important that using these parameters we can write down the effective potential at the L-loop level as

$$V^{(L)} = \lambda_1^{L-1} M_-^4 \left[\text{function of } \log\left(\frac{M_-^2}{\mu^2}\right), \log\left(\frac{M_+^2}{\mu^2}\right), P\right], \tag{15}$$

where P is the generic term of $(p_1, \ldots, p_7)$:

$$p_1 = \frac{M_+^2}{M_-^2},\ p_2 = \theta,\ p_3 = \frac{x_1^2}{M_-^2},\ p_4 = \frac{x_2^2}{M_-^2}, \tag{16}$$

$$p_5 = y_1,\ p_6 = y_2,\ p_7 = \lambda_1 \frac{\Lambda}{M_-^4}. \tag{17}$$

Let us explain why the L-loop effective potential can be written as Eq. (15). Since λ_1 can be treated like an $\hbar$ in front of the action, the L-loop effective potential is proportional to λ_1^{L-1}. The part in the square brackets $[\cdots]$ in Eq. (15) is dimensionless because M_-^4 is extracted as a dimensionful part of $V^{(L)}$. So since we introduce dimensionless parameters $(p_1, \ldots, p_7)$ based on Eqs. (10)–(14), the part in the square brackets $[\cdots]$ can be written in terms of two logarithms ($\log(M_-^2/\mu^2)$ and $\log(M_+^2/\mu^2)$) and dimensionless parameters $(p_1, \ldots, p_7)$.

As is well known, since the L-loop effective potential $V^{(L)}$ contains the Lth power of the logarithm at most, one can express $V^{(L)}$ with respect to $\log(M_-^2/\mu^2)$ and $\log(M_+^2/\mu^2)$:

$$V^{(L)} = \frac{M_-^4}{\lambda_1} \sum_{l=0}^{L} \sum_{k=0}^{L-l} \lambda_1^l v^{(L)}_{L-(k+l),k}(P) s_1^{L-(l+k)} s_2^k, \tag{18}$$

where, multiplying each logarithm by λ_1, we define s_1 and s_2:

$$s_1 = \lambda_1 \log\left(\frac{M_-^2}{\mu^2}\right), \qquad s_2 = \lambda_1 \log\left(\frac{M_+^2}{\mu^2}\right).$$

Finally, by summing up $V^{(L)}$ from $L = 0$ to $L = \infty$, we obtain the total effective potential expressed in terms of s_1 and s_2:

$$V = \sum_{L=0}^{\infty} V^{(L)} = \frac{M_-^4}{\lambda_1} \sum_{l=0}^{\infty} \lambda_1^l f_l(P, s_1, s_2), \tag{19}$$

$$f_l(P, s_1, s_2) = \sum_{L=l}^{\infty} \sum_{k=0}^{L-l} v^{(L)}_{L-(l+k),k}(P) s_1^{L-(l+k)} s_2^k. \tag{20}$$

In this expression the power of λ_1 gives the order of the leading log-series expansion. In this sense, f_l means the lth-to-leading log function of the effective potential.

Next, we consider the choice of renormalization scale. As is well known, the effective potential satisfies the RG equation

$$\mathcal{D}V = \mu \frac{d}{d\mu} V = 0, \tag{21}$$

where the RG differential operator is given as

$$\mathcal{D} = \mu \frac{d}{d\mu} = \mu \frac{\partial}{\partial \mu} - \sum_X \gamma_X X \frac{\partial}{\partial X} + \sum_Y \beta_Y \frac{\partial}{\partial Y}, \tag{22}$$

where

$$\gamma_X = -\frac{\mu}{X} \frac{dX}{d\mu}, \qquad \beta_Y = \mu \frac{dY}{d\mu},$$

$$X = m_1^2, m_2^2, \Lambda, \phi_1, \phi_2, \qquad Y = \lambda_1, \lambda_2, \lambda_3. \tag{23}$$

These specific β and γ functions are given in Appendix A. We can then obtain the solution of the RG equation as

$$V(\phi, \beta, Q; \mu_0^2) = V\left(\bar{G}(t, \beta)\phi, \beta, \bar{Q}(t); \mu_0^2 e^{2t}\right), \tag{24}$$

where we use a shorthand notation $Q(= m_1^2, m_2^2, \lambda_1, \lambda_2, \lambda_3, \Lambda)$ and introduce t to express the renormalization scale μ^2 as $\mu^2(t) = \mu_0^2 e^{2t}$. Also, $\bar{G}(\beta, t)$ is defined as

$$\begin{aligned}\bar{\phi}_1(t)^2 + \bar{\phi}_2(t)^2 &= \left(\exp\left[-2\int_0^t ds \bar{\gamma}_{\phi_1}(s)\right]\cos^2\beta + \exp\left[-2\int_0^t ds \bar{\gamma}_{\phi_2}(s)\right]\sin^2\beta\right)\phi^2 \\ &\equiv \bar{G}(\beta, t)^2\phi^2.\end{aligned} \tag{25}$$

However, because of $\gamma_{\phi_1} = \gamma_{\phi_2} = 0$, from now on, we set $\bar{G}(\beta, t) = 1$. $\bar{Q}(t)$ is the solution of β or γ function and satisfies an initial value Q at an initial renormalization scale μ_0^2 or $t = 0$. The RG solution of Eq. (24) for the effective potential means that it is independent of the renormalization scale t. Since we can freely choose the renormalization scale, we look for the best choice of it. Let us take the renormalization scale as follows:

$$\mu^2 = \bar{M}_-(t)^2. \tag{26}$$

Since this choice leads to $\bar{s}_1(t) = 0$, the RG improved effective potential expressed with Eq. (19) becomes

$$V = \bar{M}_-(t)^4 \sum_{l=0}^{\infty} \bar{\lambda}_1(t)^{l-1} f_l(\bar{P}, \bar{s}_1 = 0, \bar{s}_2),$$

where from Eq. (20)

$$f_l(\bar{P}, \bar{s}_1 = 0, \bar{s}_2) = \sum_{L=l}^{\infty} v_{0,L-l}^{(L)}(\bar{P})\bar{s}_2^{L-l}.$$

Here, if we assume $\bar{s}_2 \lesssim \mathcal{O}(\bar{\lambda}_1)$, one gets the lth-to-leading log function:

$$f_l(\bar{P}, \bar{s}_1 = 0, \bar{s}_2) = v_{0,0}^{(l)}(\bar{P}) + \mathcal{O}\left(\bar{\lambda}_1\right). \tag{27}$$

If $\bar{s}_2 \lesssim \mathcal{O}(\bar{\lambda}_1)$ and we would like to evaluate the effective potential up to Lth-to-leading log order, the expression is written as

$$\begin{aligned}V &= \bar{M}_-(t)^4 \sum_{l=0}^{L} \bar{\lambda}_1(t)^{l-1} f_l(\bar{P}, \bar{s}_1 = 0, \bar{s}_2)\Big|_{\bar{s}_2 \lesssim \mathcal{O}(\bar{\lambda}_1)} \\ &= \bar{M}_-(t)^4 \sum_{l=0}^{L} \bar{\lambda}_1(t)^{l-1} v_{0,0}^{(l)}(\bar{P})\Big|_{\mu^2 = \bar{M}_-^2} + \mathcal{O}\left(\bar{\lambda}_1^L\right) \\ &= \sum_{l=0}^{L} V^{(l)}(\phi, \beta, \bar{Q}(t); \mu_0^2 e^{2t})\Big|_{\mu^2 = \bar{M}_-^2} + \mathcal{O}\left(\bar{\lambda}_1^L\right).\end{aligned} \tag{28}$$

We notice that the term of $\mathcal{O}\left(\bar{\lambda}_1\right)$ in Eq. (27) contributes to the effective potential beyond the Lth-to-leading log order. Note that the RG improved effective potential is exactly correct up to Lth-to-leading log order only if the RG equations for the parameters are solved up to the $(L+1)$ loop level. In summary, if one prepares the L-loop effective potential and $(L+1)$-loop β and γ functions, one can construct the RG improved effective potential (28) up to Lth-to-leading log order for the case of $\bar{s}_2 \lesssim \mathcal{O}\left(\bar{\lambda}_1\right)$.

We comment on the variables of the effective potential. Originally, the effective potential has three variables (ϕ, β, t). However, now that $\mu(t)^2$ is taken to be equal to $\bar{M}_-(\phi,\beta,t)^2$, these variables are related. In our paper, we show that we can solve $\mu(t)^2 = \bar{M}_-(\phi,\beta,t)^2$ analytically with respect to ϕ and construct the RG improved effective potential by using the solution of ϕ.[2]

Since the above prescription is correct only in the case of $\bar{s}_2 \lesssim \mathcal{O}\left(\bar{\lambda}_1\right)$, we must consider the method of the RG improvement for the case of $\bar{s}_2 > \mathcal{O}\left(\bar{\lambda}_1\right)$. In that case, as seen from the logarithm $\log\left(\bar{M}_+(t)^2/\bar{M}_-(t)^2\right)$ of $\bar{s}_2$, the relative magnitude of the mass eigenvalues is large. In such a case, we make use of the decoupling theorem [25]. The decoupling of the heavy particle means that the logarithm of the particle is absorbed into the parameters defined in the effective theory. The remaining logarithm is only one of a light particle. If the theory includes only a single logarithm, by setting the renormalization scale as the light mass, the RG improved effective potential can be calculated. We discuss this situation more specifically in Sect. 4.

3. RG improved effective potential in a two real scalar system (massless case)

We specifically calculate the RG improved effective potential by the method constructed in Sect. 2. In this section we treat the two real scalar model without mass parameters. The procedure for the construction of the RG effective potential is as follows. Because of taking the renormalization scale as $\mu_0^2 e^{2t} = \bar{M}_-(t)^2$, we solve it with respect to ϕ. Substituting the ϕ into the mass eigenvalue M_+^2 and the effective potential, we can evaluate $\log(\bar{M}_+(t)^2/\bar{M}_-(t)^2)$ and the effective potential. If the logarithm is small enough for $\bar{s}_2$ to be of the order of $\bar{\lambda}_1$, we can use the expression of Eq. (28) as the effective potential up to Lth-to-leading log order.

In order to obtain ϕ with $\mu_0^2 e^{2t} = \bar{M}_-(t)^2$ satisfied, we solve it in terms of ϕ. In the present model, the mass eigenvalues $M_\pm^2$ are written as

$$\begin{aligned} M_\pm^2 &= \frac{\phi^2}{4}\Big((\lambda_1+\lambda_3)\cos^2\beta + (\lambda_3+\lambda_2)\sin^2\beta \\ &\qquad \pm \sqrt{\left((\lambda_1-\lambda_3)\cos^2\beta + (\lambda_3-\lambda_2)\sin^2\beta\right)^2 + 16\lambda_3^2\sin^2\beta\cos^2\beta}\Big) \\ &\equiv \lambda_\pm(\beta)\phi^2. \end{aligned}$$

So we can easily obtain ϕ from $\mu_0^2 e^{2t} = \bar{M}_-(t)^2$:

$$\phi^2 = \frac{\mu_0^2 e^{2t}}{\bar{\lambda}_-(\beta,t)}. \tag{29}$$

[2] Moreover, note that although the dimensionless parameters P are introduced for the derivation of the logarithmic structure of the effective potential, the final expression is written in terms of the parameters Q. Namely, we do not use the dimensionless parameters P but the parameters Q for the calculation of the RG improved effective potential (28) .

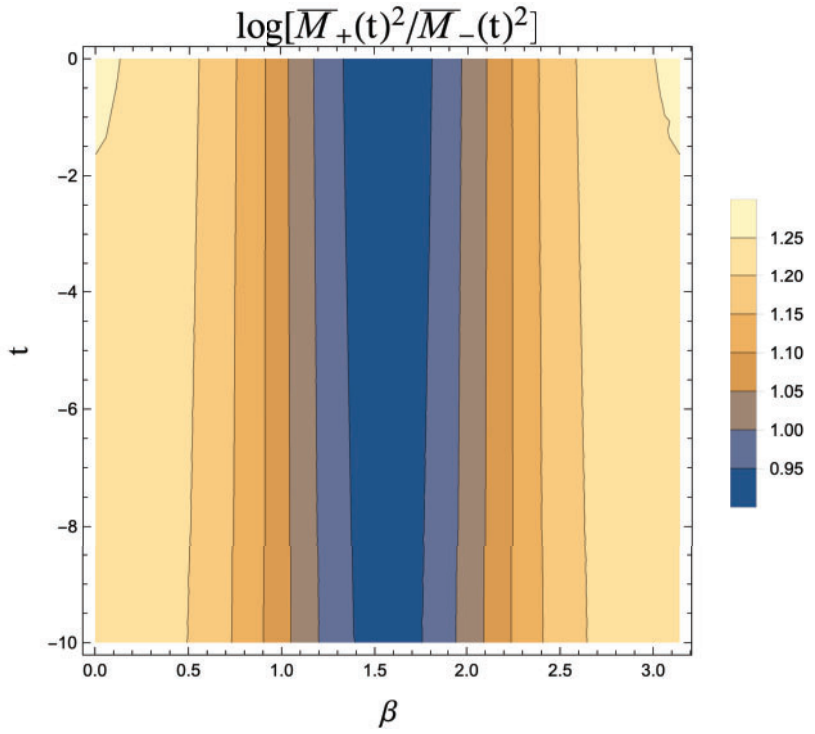

Fig. 1. A contour plot of $\log(\bar{M}_+^2/\bar{M}_-^2)$ in the regions of $\beta \in (0,\pi)$ and $t \in (-10,0)$. We take $\lambda_1 = 0.7$, $\lambda_2 = 0.5$, $\lambda_3 = 0.2$, and $\phi = 10$ at $\mu_0^2 = M_-^2$ as an initial condition.

As mentioned above, now ϕ is not the variable of the effective potential and is determined by β and t. The ϕ appearing in the mass eigenvalue $\bar{M}_+^2$ and the effective potential is calculated with Eq. (29).

The logarithm of $\bar{s}_2$ is written as

$$\log\left(\frac{\bar{M}_+(t)^2}{\mu(t)^2}\right)\Bigg|_{\mu(t)^2=\bar{M}_-(t)^2} = \log\left(\frac{\bar{\lambda}_+(\beta,t)}{\bar{\lambda}_-(\beta,t)}\right), \tag{30}$$

where ϕ is canceled out because of the massless model. At this stage we assign initial values of (λ_1, λ_2, λ_3) for performing the numerical calculation. Taking $\lambda_1 = 0.7, \lambda_2 = 0.5, \lambda_3 = 0.2$, and $\phi = 10$ at $\mu_0^2 = M_-^2$, we calculate $\log(\bar{M}_+(t)^2/\bar{M}_-(t)^2)$ for the range of $\beta \in (0,\pi)$ and $t \in (-10,0)$ by 1-loop β functions in Fig. 1. In Fig. 1 we see that $\log(\bar{M}_+(t)^2/\bar{M}_-(t)^2) \approx 1$ in the regions of (β,t). Thus, since we can conclude that $\bar{s}_2 \approx \bar{\lambda}_1$, Eq. (28) can be used as the RG improved effective potential. Using the tree-level effective potential and the 1-loop β function, the RG improved effective potential at the leading log order is given as

$$V = \left(\frac{\bar{\lambda}_1(t)}{4!}\cos^4\beta + \frac{\bar{\lambda}_2(t)}{4!}\sin^4\beta + \frac{\bar{\lambda}_3(t)}{4}\sin^2\beta\cos^2\beta\right)\phi^4 \quad \text{with} \quad \phi^2 = \frac{\mu_0^2 e^{2t}}{\bar{\lambda}_-(\beta,t)}, \tag{31}$$

where the condition for ϕ^2 originates from the choice of the renormalization scale $\mu^2 = \bar{M}_-(t)^2$, as seen in Eq. (29). Clearly the RG improved effective potential is determined by β and t. In Fig. 2, the RG improved effective potential is plotted as axes of $(\phi_1/\mu_0, \phi_2/\mu_0)$ for the regions of $\beta \in (0,\pi)$ and $t \in (-10,0)$.

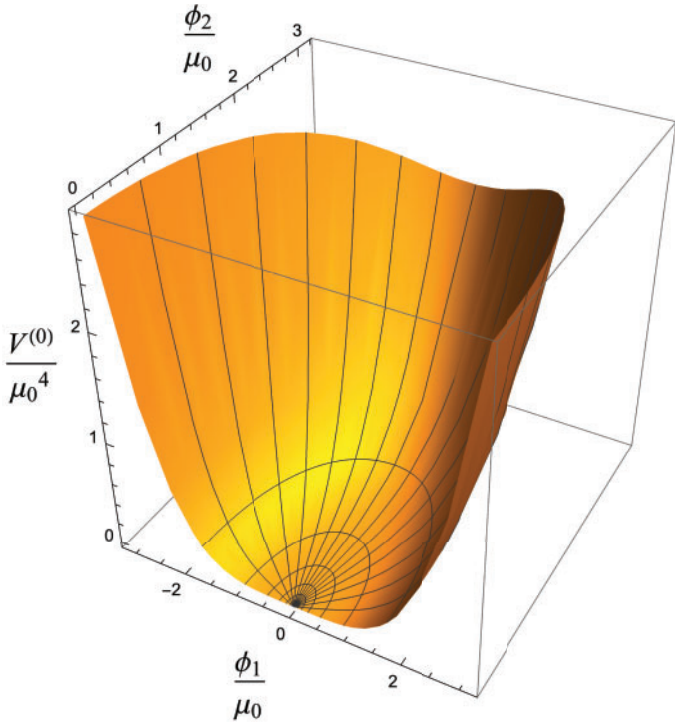

Fig. 2. A 3D plot of the RG improved effective potential at the leading log order divided by the initial renormalization scale μ_0^4 as axes of $(\phi_1/\mu_0, \phi_2/\mu_0)$. This is plotted in the regions of $\beta \in (0, \pi)$ and $t \in (-10, 0)$. The initial condition is the same as in Fig. 1.

4. RG improved effective potential in a two real scalar system (massive case)

In this section we consider the massive theory in a two real scalar model. In particular, we treat the effective potential causing spontaneous symmetry breaking. The procedure for the construction of the RG improved effective potential is the same as the previous method. We solve Eq. (26) for ϕ in the massive case. In this case, because of the mass parameters, the equation is a little complicated but it can be analytically solved. Equation (26) is written as follows:

$$A = \sqrt{B}, \tag{32}$$

where

$$A = m_1^2 + m_2^2 - 2\mu^2 + \frac{1}{2}\Big((\lambda_1 + \lambda_3)\cos^2\beta + (\lambda_2 + \lambda_3)\sin^2\beta\Big)\phi^2,$$

$$B = \left\{m_1^2 - m_2^2 + \frac{1}{2}\Big((\lambda_1 - \lambda_3)\cos^2\beta + (\lambda_3 - \lambda_2)\sin^2\beta\Big)\phi^2\right\}^2 + 4\lambda_3^2\sin^2\beta\cos^2\beta\phi^4.$$

Squaring both sides of $A = \sqrt{B}$, a quadratic equation for ϕ^2 is given as

$$a\phi^4 + 2b\phi^2 + c = 0, \tag{33}$$

where

$$a = \lambda_1\lambda_3\cos^4\beta + \lambda_2\lambda_3\sin^4\beta + (\lambda_1\lambda_2 - 3\lambda_3^2)\sin^2\beta\cos^2\beta,$$

$$b = (\lambda_3 \cos^2\beta + \lambda_2 \sin^2\beta)(m_1^2 - \mu^2) + (\lambda_1 \cos^2\beta + \lambda_3 \sin^2\beta)(m_2^2 - \mu^2),$$
$$c = 4(m_1^2 - \mu^2)(m_2^2 - \mu^2).$$

We can obtain the solution ϕ^2 as

$$\phi^2 = \frac{-b \pm \sqrt{b^2 - ac}}{a}. \tag{34}$$

Since we solve the quadratic equation, there are two solutions for ϕ^2. However, because the original equation is $A = \sqrt{B}$, the solution satisfies the following conditions:

$$A > 0 \quad \text{and} \quad B > 0. \tag{35}$$

Although it is difficult to analytically prove whether either solution satisfies the condition or not, by using the initial values as inputs in the following subsections we confirm numerically the following results:

$$\phi^2 = \frac{-b + \sqrt{b^2 - ac}}{a} \quad \rightarrow \quad A > 0 \quad \text{and} \quad B > 0,$$
$$\phi^2 = \frac{-b - \sqrt{b^2 - ac}}{a} \quad \rightarrow \quad A < 0 \quad \text{and} \quad B < 0.$$

Therefore we adopt the solution ϕ as

$$\phi^2 = \frac{-b + \sqrt{b^2 - ac}}{a}. \tag{36}$$

Since we get the solution ϕ for Eq. (26), we can construct the RG improved effective potential. The expression is provided at leading log order as

$$V = \frac{1}{2}(\bar{m}_1(t)^2 \cos^2\beta + \bar{m}_2(t)^2 \sin^2\beta)\phi^2 + \frac{1}{4!}(\bar{\lambda}_1(t)\cos^4\beta + \bar{\lambda}_2(t)\sin^4\beta + 6\bar{\lambda}_3(t)\sin^2\beta\cos^2\beta)\phi^4 + \bar{\Lambda}(t)$$
$$\text{with} \qquad \phi^2 = \frac{-\bar{b}(\beta,t) + \sqrt{\bar{b}(\beta,t)^2 - \bar{a}(\beta,t)\bar{c}(t)}}{\bar{a}(\beta,t)}. \tag{37}$$

In the following subsections, we consider two situations for inputting the initial value of the renormalization scale. First, taking $(m_1^2 < 0, m_2^2 < 0, -m_1^2 \sim -m_2^2)$ as the mass parameters, we set the initial renormalization scale on the vacuum, which is determined by the stationary condition of the effective potential. Increasing the renormalization scale from the low-energy scale at the vacuum, we analyze the behavior of the RG improved effective potential in the high-energy region. Second, we input the initial values of the parameters on the high-energy scale and decrease the renormalization scale to the low-energy scale. Assuming $(m_1^2 < 0, m_2^2 > 0, -m_1^2 \ll m_2^2)$ for the mass parameters, we investigate the RG improved effective potential in the low-energy region. As the renormalization scale decreases, the mass eigenvalue $\bar{M}_-^2$ also declines and reaches m_2^2 at a scale. Since $\bar{M}_-^2$ continues to decline below the scale, we find the logarithm of $\bar{s}_2$ large. In order to avoid the breakdown of the logarithmic perturbation, we utilize the decoupling theorem. Applying the decoupling theorem, we derive the RG improved effective potential in the low-energy scale and visualize the behavior including the minimum value of the RG improved effective potential.

4.1. $-m_2^2 \sim -m_1^2$

Since we set the initial condition on the vacuum in this subsection, we derive the stationary condition for the effective potential. Introducing a convenient notation for the mass parameter and quartic coupling constant:

$$m(\beta)^2 = m_1^2 \cos^2\beta + m_2^2 \sin^2\beta,$$
$$\lambda(\beta) = \lambda_1 \cos^4\beta + \lambda_2 \sin^4\beta + 6\lambda_3 \sin^2\beta \cos^2\beta,$$

we can write the effective potential at a tree level:

$$V^{(0)} = \frac{m(\beta)^2}{2}\phi^2 + \frac{\lambda(\beta)}{4!}\phi^4 + \Lambda.$$

We calculate the stationary conditions for the effective potential:

$$\frac{\partial V^{(0)}}{\partial \phi} = 0, \quad \frac{\partial V^{(0)}}{\partial \beta} = 0. \tag{38}$$

From $\frac{\partial V^{(0)}}{\partial \phi} = 0$, we derive the following condition:

$$\phi^2 = -6\frac{m(\beta)^2}{\lambda(\beta)}. \tag{39}$$

Combining this condition and $\frac{\partial V^{(0)}}{\partial \beta} = 0$, we get the stationary condition for β:

$$\beta = \arccos\left[\frac{\lambda_2 m_1^2 - 3\lambda_3 m_2^2}{(\lambda_2 - 3\lambda_3)m_1^2 + (\lambda_1 - 3\lambda_3)m_2^2}\right]. \tag{40}$$

Substituting this β for Eq. (39), we can obtain ϕ on the stationary point:

$$\phi^2 = -6\frac{(\lambda_2 - 3\lambda_3)m_1^2 + (\lambda_1 - 3\lambda_3)m_2^2}{\lambda_1\lambda_2 - 9\lambda_3^2}. \tag{41}$$

Using Eqs. (41)–(40), we can calculate the vacuum expectation value and also estimate the initial renormalization scale $\mu_0^2 = \bar{M}_-(t=0)^2 = M_-^2$. For simplicity, in this section we impose $\Lambda = 0$ at the initial point.

Taking [$\lambda_1 = 0.7$, $\lambda_2 = 0.5$, $\lambda_3 = 0.1$, $m_1^2 = -(160\ \text{GeV})^2$, and $m_2^2 = -(170\ \text{GeV})^2$] as an initial condition, we get the vacuum expectation value $(\phi, \beta) = (591\ \text{GeV}, 0.94)$, the initial renormalization scale $\mu_0 = M_- = 135$ GeV, and the mass eigenvalue $M_+ = 236$ GeV. We regard the vacuum expectation value and the initial renormalization scale as a starting point for the RG improved effective potential and the running parameters. Then, we run $\log(\bar{M}_+(t)^2/\bar{M}_-(t)^2)$ by the RG equations in the regions of $t \in (0, 5)$ and $\beta \in (0, \frac{\pi}{2})$. Figure 3 shows the result of the logarithm. On $\beta = 0$ and $\beta = \frac{\pi}{2}$ in Fig. 3, the logarithm takes 2–3 in the range of $t = (0, 2)$ and less than 2 for $t > 2$. In $\beta = \frac{\pi}{4}$, the logarithm is less than 1 for the whole scale of t. If the magnitude of the logarithm as $\log(\bar{M}_-^2/\bar{M}_+^2) \lesssim 3$ is accepted in the context of a logarithmic perturbative expansion, the RG improved effective potential is calculated with Eq. (37). The result is shown in Fig. 4. In the left panel of Fig. 4, the dot-dashed green, dotted orange, and solid blue lines correspond to the RG improved effective potential in $\beta = 0$, $\beta = \frac{\pi}{4}$, and $\beta = \frac{\pi}{2}$, respectively. In the right panel of Fig. 4, the dot-dashed green, dotted orange, and solid blue lines correspond to ϕ in $\beta = 0$, $\beta = \frac{\pi}{4}$, and

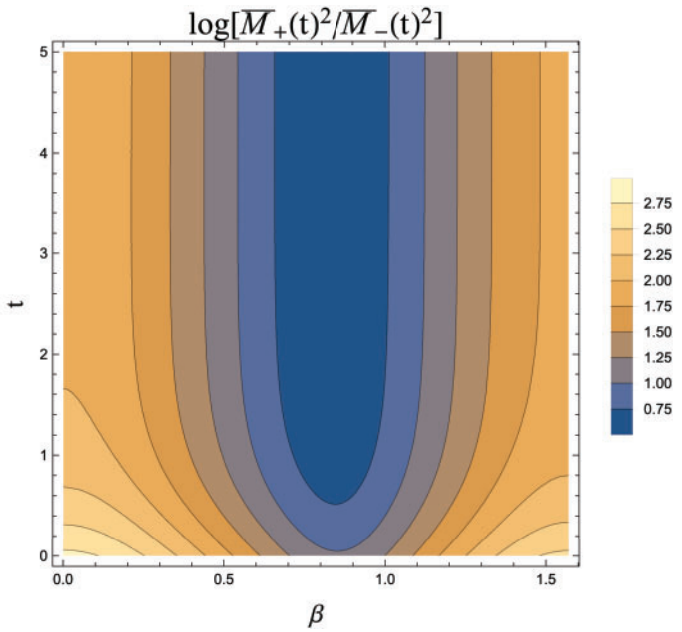

Fig. 3. The logarithm of the ratio of $\bar{M}_+(t)^2$ to $\bar{M}_-(t)^2$ is plotted in the ranges of $\beta \in (0, \frac{\pi}{2})$ and $t \in (0, 5)$. The result is produced by taking $\lambda_1 = 0.7$, $\lambda_2 = 0.5$, $\lambda_3 = 0.1$, $m_1^2 = -(160\ \text{GeV})^2$, and $m_2^2 = -(170\ \text{GeV})^2$ as an initial condition for the RG equation.

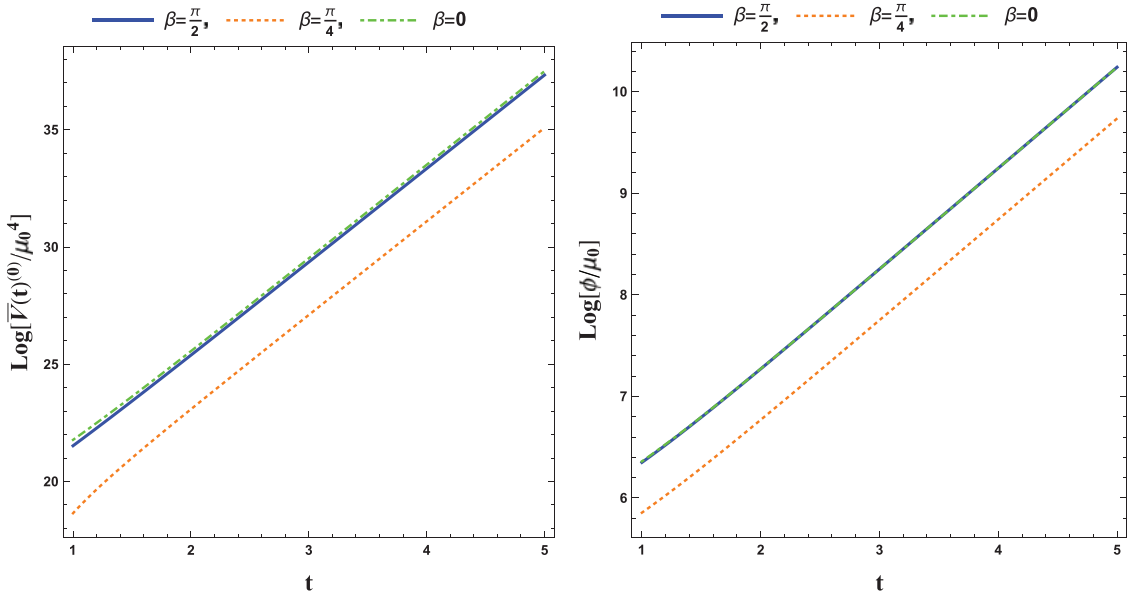

Fig. 4. Left: The dot-dashed green, dotted orange, and solid blue lines correspond to the RG improved effective potential in $\beta = 0$, $\beta = \frac{\pi}{4}$, and $\beta = \frac{\pi}{2}$, respectively. Right: The dot-dashed green, dotted orange, and solid blue lines correspond to ϕ in $\beta = 0$, $\beta = \frac{\pi}{4}$, and $\beta = \frac{\pi}{2}$, respectively. The initial condition for the RG equation is the same as in Fig. 3.

$\beta = \frac{\pi}{2}$, respectively (ϕ in $\beta = 0$ and $\frac{\pi}{2}$ are ϕ_1 and ϕ_2, respectively). In both panels of Fig. 4, the lines at $\beta = 0$ and $\frac{\pi}{2}$ overlap with each other.

We give a more complete discussion for the logarithmic perturbative expansion. As explained above, there are regions in which the logarithm is beyond 1. If the logarithm is considered to be large, the heavy field with mass $\bar{M}_+$ should be decoupled from the theory. Due to this decoupling,

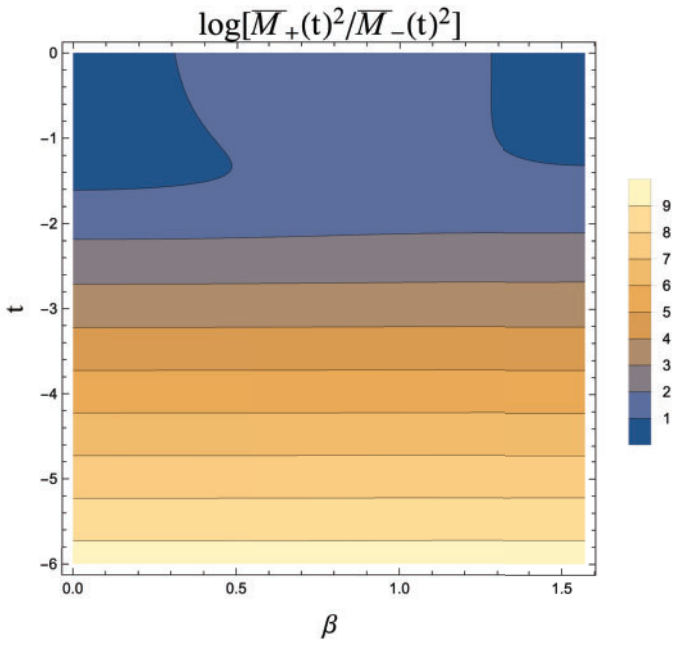

Fig. 5. The logarithm of the ratio of $\bar{M}_+(t)^2$ to $\bar{M}_-(t)^2$ is plotted in the regions of $\beta \in (0, \frac{\pi}{2})$ and $t \in (-6, 0)$. The initial condition is given as $\lambda_1 = 0.7, \lambda_2 = 0.6, \lambda_3 = 0.4, m_1^2 = -(200\ \text{GeV})^2, m_2^2 = (3000\ \text{GeV})^2, \Lambda = 0$ at $(\phi, \beta) = (40\,000\ \text{GeV}, \frac{\pi}{4})$.

the remaining logarithm is only $\log(\bar{M}_-^2/\mu^2)$. Since the single logarithm can be suppressed by using the degree of freedom of the renormalization scale μ, the logarithmic perturbation is stable. Such a procedure is explained in the next subsection.

4.2. $m_2^2 \gg -m_1^2$

In this subsection we impose the initial condition at a high-energy scale and gradually decrease the renormalization scale to a scale around $-m_1^2$. Also we suppose that $m_2^2 \gg -m_1^2 > 0$. Setting the following initial condition:

$$\lambda_1 = 0.7,\ \lambda_2 = 0.6,\ \lambda_3 = 0.4,$$
$$m_1^2 = -(200\ \text{GeV})^2,\ m_2^2 = (3000\ \text{GeV})^2,\ \Lambda = 0,$$

at $(\phi, \beta) = (40\,000\ \text{GeV}, \frac{\pi}{4})$, we evaluate the logarithm of the ratio of $\bar{M}_+(t)^2$ to $\bar{M}_-(t)^2$ in Fig. 5. Clearly, the logarithm becomes large as the renormalization scale decreases to the low-energy scale. This indicates the breakdown of the logarithmic perturbative expansion in the low-energy region. For more detail, we evaluate the ratio of $\bar{M}_-(t)^2$ to $\bar{m}_2(t)^2$ in the left panel of Fig. 6. As seen from the left panel in Fig. 6, $\bar{M}_-(t)$ steadily falls with decreasing renormalization scale t. The ratio of $\bar{M}_+(t)^2$ to m_2^2 is calculated in the right panel of Fig. 6. In contrast to the figure on the left, the figure shows that the value of $\bar{M}_+(t)$ is comparable to $\bar{m}_2(t)$ below $t = -1$. Therefore in Fig. 6 we find out that the ratio of $\bar{M}_+(t)^2$ to $\bar{M}_-(t)^2$ increases with lower renormalization scale because $\bar{M}_-(t)$ is smaller than $\bar{m}_2(t)$ while $\bar{M}_+(t)$ is comparable to $\bar{m}_2(t)$.

In order to avoid a large logarithm, we should modify the RG improved effective potential for the low-energy scale. The way to modify the RG improvement is to utilize the decoupling theorem. In the present case, since $\bar{M}_+(t)$ is heavier than $\bar{M}_-(t)$, the field with the mass $\bar{M}_+(t)$ should be decoupled. Moreover, as seen in the right panel of Fig. 6, since $\bar{M}_+(t)$ is comparable to $\bar{m}_2(t)$, we

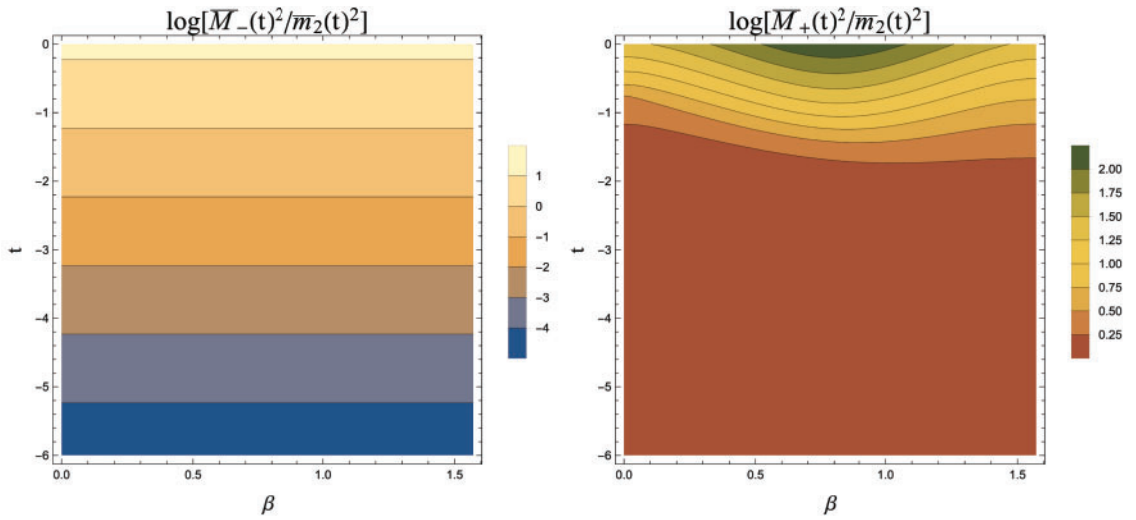

Fig. 6. Left: The logarithm of the ratio of $\bar{M}_-(t)^2$ to $\bar{m}_2(t)^2$ is evaluated in the regions of $\beta \in (0, \frac{\pi}{2})$ and $t \in (-6, 0)$. Right: The logarithm of the ratio of $\bar{M}_+(t)^2$ to $\bar{m}_2(t)^2$ is calculated in the regions of $\beta \in (0, \frac{\pi}{2})$ and $t \in (-6, 0)$.

factor out $\bar{m}_2(t)^2$ from the expression of $\bar{M}_+(t)^2$. Hereafter we omit the bar of the parameters to reduce the bother. To implement it, we expand M_+^2 with respect to $\frac{\phi^2}{m_2^2}$:

$$M_+^2 = m_2^2(1+\Delta),$$
$$\Delta = \left(\frac{\lambda_3}{2}\cos^2\beta + \frac{\lambda_2}{2}\sin^2\beta\right)\frac{\phi^2}{m_2^2} + \lambda_3^2\sin^2\beta\cos^2\beta\left(\frac{\phi^4}{m_2^4}\right).$$

Additionally, we expand the 1-loop effective potential with M_+^2 in terms of $\frac{\phi^2}{m_2^2}$:

$$\begin{aligned} V_+^{(1)} &= \frac{M_+^4}{64\pi^2}\left(\log\left(\frac{M_+^2}{\mu^2}\right) - \frac{3}{2}\right) \\ &= \frac{m_2^4}{64\pi^2}\left(\log\left(\frac{m_2^2}{\mu^2}\right) - \frac{3}{2}\right) + \frac{m_2^2}{64\pi^2}(\lambda_3\cos^2\beta + \lambda_2\sin^2\beta)\left(\log\left(\frac{m_2^2}{\mu^2}\right) - 1\right)\phi^2 \\ &\quad + \frac{1}{64\pi^2}\left\{2\lambda_3^2\sin^2\beta\cos^2\beta\left(\log\left(\frac{m_2^2}{\mu^2}\right) - 1\right) + \frac{1}{4}\left(\lambda_3\cos^2\beta + \lambda_2\sin^2\beta\right)^2\log\left(\frac{m_2^2}{\mu^2}\right)\right\}\phi^4 \\ &\quad + \mathcal{O}\left(\frac{\phi^6}{m_2^2}\right). \end{aligned} \tag{42}$$

In this expression we see that $\log(m_2^2/\mu^2)$ leads to a large logarithm, which is not suppressed with the choice of $\mu^2 = M_-^2$. The concept of the decoupling theorem is to absorb the large logarithm into new parameters by the redefinition of the parameters. Hence we combine the 1-loop effective potential with the tree effective potential and redefine the new parameters to renormalize the large logarithm:

$$V^{(0)} + V_+^{(1)} = \frac{\phi^2}{2}(\tilde{m}_1^2\cos^2\beta + \tilde{m}_2^2\sin^2\beta)$$

$$+\frac{\phi^4}{4!}(\tilde{\lambda}_1\cos^4\beta+\tilde{\lambda}_2\sin^4\beta+6\tilde{\lambda}_3\sin^2\beta\cos^2\beta)+\tilde{\Lambda}, \tag{43}$$

where

$$\tilde{m}_1^2=m_1^2+\frac{\lambda_3 m_2^2}{32\pi^2}\left(\log\left(\frac{m_2^2}{\mu^2}\right)-1\right), \tag{44}$$

$$\tilde{m}_2^2=m_2^2+\frac{\lambda_2 m_2^2}{32\pi^2}\left(\log\left(\frac{m_2^2}{\mu^2}\right)-1\right), \tag{45}$$

$$\tilde{\lambda}_1=\lambda_1+\frac{3\lambda_3^2}{32\pi^2}\log\left(\frac{m_2^2}{\mu^2}\right), \tag{46}$$

$$\tilde{\lambda}_2=\lambda_2+\frac{3\lambda_2^2}{32\pi^2}\log\left(\frac{m_2^2}{\mu^2}\right), \tag{47}$$

$$\tilde{\lambda}_3=\lambda_3+\frac{\lambda_3^2}{8\pi^2}\left(\log\left(\frac{m_2^2}{\mu^2}\right)-1\right)+\frac{\lambda_2\lambda_3}{32\pi^2}\log\left(\frac{m_2^2}{\mu^2}\right), \tag{48}$$

$$\tilde{\Lambda}=\Lambda+\frac{m_2^4}{64\pi^2}\left(\log\left(\frac{m_2^2}{\mu^2}\right)-\frac{3}{2}\right). \tag{49}$$

Note that because there is no contribution to the wavefunction renormalization in this model, the classical background fields do not change:

$$\tilde{\phi}_1=\phi_1, \qquad \tilde{\phi}_2=\phi_2. \tag{50}$$

Since we use the parameters in the low-energy effective theory below $\mu^2=m_2^2$, we derive the β and γ functions for the redefined parameters. To derive them, the RG differential operator in Eq. (22) is rewritten in terms of the new parameters:

$$\begin{aligned}\mathcal{D}=\mu\frac{d}{d\mu}&=(\mathcal{D}\mu)\frac{\partial}{\partial\mu}+\sum_{\tilde{X}}(\mathcal{D}\tilde{X})\frac{\partial}{\partial\tilde{X}}+\sum_{\tilde{Y}}(\mathcal{D}\tilde{Y})\frac{\partial}{\partial\tilde{Y}},\\&=\mu\frac{\partial}{\partial\mu}-\sum_{\tilde{X}}\gamma_{\tilde{X}}\tilde{X}\frac{\partial}{\partial\tilde{X}}+\sum_{\tilde{Y}}\beta_{\tilde{Y}}\frac{\partial}{\partial\tilde{Y}},\end{aligned} \tag{51}$$

where

$$\tilde{X}=\tilde{m}_1^2,\tilde{m}_2^2,\tilde{\Lambda},\tilde{\phi}_1,\tilde{\phi}_2, \qquad \tilde{Y}=\tilde{\lambda}_1,\tilde{\lambda}_2,\tilde{\lambda}_3. \tag{52}$$

Hence we can get the β and γ functions defined by the tilde parameters:

$$\beta_{\tilde{\lambda}_1}=\frac{3\tilde{\lambda}_1^2}{16\pi^2}, \qquad \beta_{\tilde{\lambda}_2}=\frac{3\tilde{\lambda}_3^2}{16\pi^2}, \qquad \beta_{\tilde{\lambda}_3}=\frac{\tilde{\lambda}_1\tilde{\lambda}_3}{16\pi^2}, \tag{53}$$

$$\gamma_{\tilde{m}_1^2}=-\frac{\tilde{\lambda}_1}{16\pi^2}, \qquad \gamma_{\tilde{m}_2^2}=-\frac{\tilde{\lambda}_3\tilde{m}_1^2}{16\pi^2\tilde{m}_2^2}, \qquad \gamma_{\tilde{\Lambda}}=-\frac{\tilde{m}_1^4}{32\pi^2\tilde{\Lambda}} \tag{54}$$

$$\gamma_{\tilde{\phi}_1}=0, \qquad \gamma_{\tilde{\phi}_2}=0. \tag{55}$$

We notice that the effect of the heavy field disappears from the RG equation in Eqs. (53)–(55). In this sense the heavy field is decoupled from theory in the low-energy scale. We can construct the RG

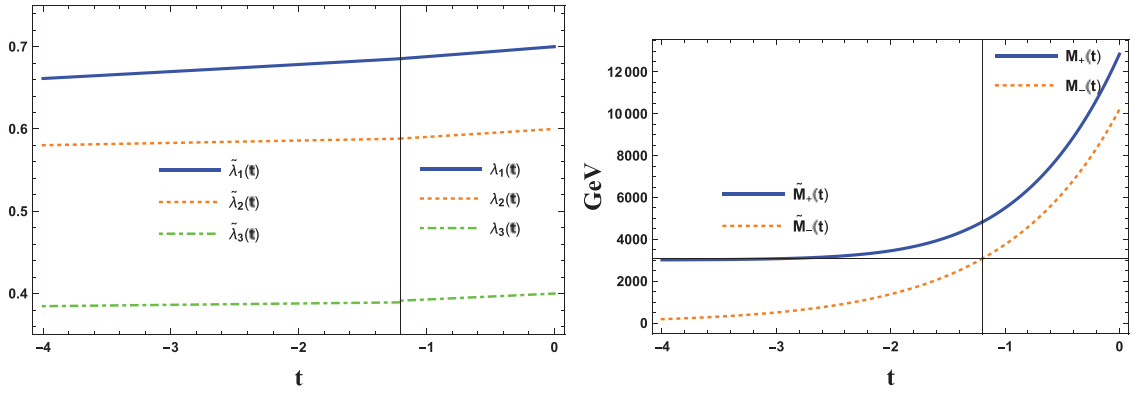

Fig. 7. Left: The running of the quartic coupling constants is solved. The solid blue, dotted orange, and dot-dashed green lines denote the running of λ_1, λ_2, and λ_3, respectively. The vertical line is the decoupling scale with $t = -1.2$. Right: The dependence of the mass eigenvalues (M_-^2, M_+^2) on the renormalization scale t is plotted.

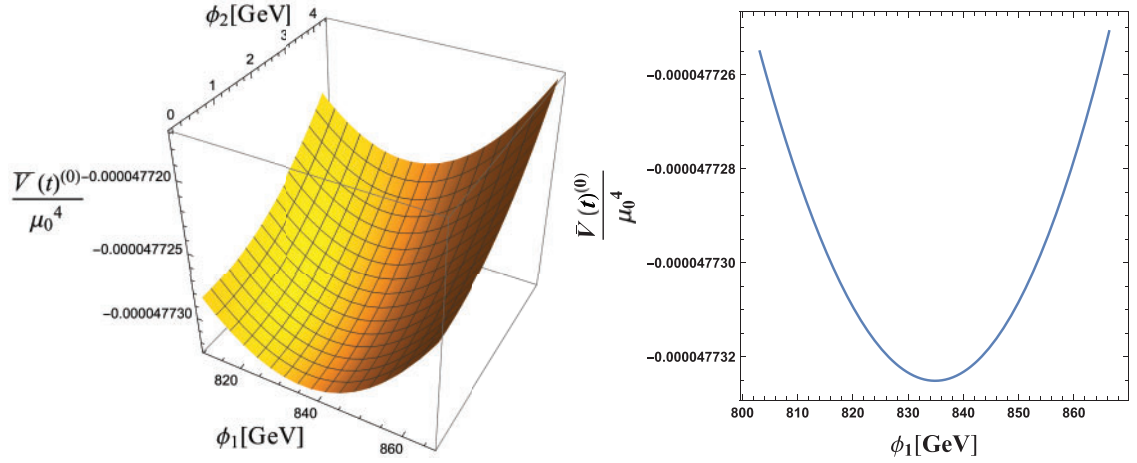

Fig. 8. Left: The 3D plot of the RG improved effective potential is evaluated as a function of (ϕ_1, ϕ_2). Right: The RG improved effective potential is plotted as a function of ϕ_1 with ϕ_2 equal to zero ($\phi_2 = 0$). From the minimum point of the RG improved effective potential, the vacuum expectation value is estimated as $(\beta = 0, t = -3.25)$.

improved effective potential by replacing the parameters with the tilde parameters for the effective potential in Eq. (37).

Let us consider a decoupling point at which the theory is separated into the full theory and the low-energy effective theory. From the left panel of Fig. 6, we see that $\bar{M}_-(t)$ coincides with $\bar{m}_2(t)$ around $t = -1$. Actually, as we can identify the scale as $t = -1.2$ and $\bar{M}_-(t)$ do not vary in the range of $\beta \in (0, \frac{\pi}{2})$, we use $(\beta, t) = (\frac{\pi}{2}, -1.2)$ as a decoupling point. The choice of the decoupling point is valid because the logarithm in Eqs. (44)–(50) is suppressed at the scale when $\bar{M}_-(t)$ becomes equal to $\bar{m}_2(t)$. Now we can solve the RG equations for all the parameters from the initial scale to the low-energy scale. In the left panel of Fig. 7, the quartic coupling constants are solved from $t = 0$ to $t = -4$. We can confirm the slight threshold correction for $\bar{\lambda}_3$. The difference between $\bar{\lambda}_3(t = -1.2)$ and $\bar{\tilde{\lambda}}_3(t = -1.2)$ normalized by $\bar{\lambda}_3(t = -1.2)$ is 0.02. In the right panel of Fig. 7, we run the mass eigenvalues in the same range. The $\bar{\tilde{M}}_-^2$ continues to decrease as the renormalization scale is lowered, while the $\bar{\tilde{M}}_+^2$ converges to about 3000 GeV. In the left panel of Fig. 8, the RG improved

effective potential is plotted as a function of (ϕ_1, ϕ_2). We can find the minimum value of the RG improved effective potential. This point corresponds to the vacuum in the present model. The right panel of Fig. 8 shows the behavior of the RG improved effective potential as a function of ϕ_1 with ϕ_2 equal to zero ($\phi_2 = 0$). From the evaluation of the RG improved effective potential, the vacuum expectation value corresponds to $(\beta, t) = (0, -3.25)$. Substituting them into the mass eigenvalues, we obtain the values of the masses:

$$\bar{\tilde{M}}_-\Big|_{\substack{\beta=0\\ t=-3.25}} = 396 \text{ GeV}, \qquad \bar{\tilde{M}}_+\Big|_{\substack{\beta=0\\ t=-3.25}} = 3007 \text{ GeV}. \tag{56}$$

5. Summary and discussion

In this paper we have studied the RG improvement of the effective potential in a two real scalar system. In Sect. 2 we clarify the logarithmic structure of the effective potential. If we choose $\mu_0^2 e^{2t} = \bar{M}_-^2(t)$ as a renormalization scale and the logarithm of $\bar{s}_2$ is less than $\mathcal{O}(1)$, we find that the RG improved effective potential up to Lth-to-leading log order can be calculated by an L-loop effective potential and $(L+1)$-loop β and γ functions. In Sects. 3 and 4, we solve $\mu_0^2 e^{2t} = \bar{M}_-^2(t)$ with respect to ϕ. This means that ϕ is not a variable of the effective potential but becomes a function of β and t. By using ϕ we can evaluate the mass eigenvalue $\bar{M}_+^2$ and the RG improved effective potential. Then, we examine if the logarithm of the ratio of $\bar{M}_+(t)^2$ to $\bar{M}_-(t)^2$ satisfies $\bar{s}_2 \lesssim \mathcal{O}(\bar{\lambda}_1)$. If it is satisfied, the RG improved effective potential can be obtained as mentioned above. On the other hand, if $\bar{s}_2 > \mathcal{O}(\bar{\lambda}_1)$, the heavy particle should be decoupled. In Sect. 4, we study such a situation. We absorb the large logarithm into the new parameters defined in the low-energy scale and derive the RG equations described in terms of the redefined parameters. The RG improved effective potential can then be constructed in the low-energy region.

There are three features in this method. First, we do not need to change the choice of the renormalization scale beyond the leading log order. This is because, since we analyze the logarithmic structure of the effective potential at any loop order, the choice $\mu_0^2 e^{2t} = \bar{M}_-(t)^2$ is valid for the RG improvement up to arbitrary lth-to-leading log order. Due to this, the ϕ that satisfies $\mu_0^2 e^{2t} = \bar{M}_-^2(t)$ is the same as the one in the leading log order. So we do not need to resolve $\mu_0^2 e^{2t} = \bar{M}_-(t)^2$ with respect to ϕ. Note that the RG equations must be solved in a loop level corresponding to the desired leading log order. Second, we can derive the RG improved effective potential without introducing multiple renormalization scales or a step function by which the heavy particle is automatically decoupled. Third, we can decouple the heavy particle from the theory by expanding the quantum correction to the effective potential with respect to ϕ^2/m^2. If the logarithm $\log\left(\phi^2/m^2\right)$ is absorbed into the parameters in the low-energy scale, we can derive the RG improved effective potential.

Our method can be applied to other multiple scalar models. If multiple scalar fields are introduced in a model, one represents the classical background fields in terms of polar coordinates such as $(\phi_1, \phi_2) = (\phi\cos\beta, \phi\sin\beta)$. With $\mu_0^2 e^{2t} = \bar{M}_{\text{lightest}}(t)^2$ chosen as a renormalization scale, the ϕ corresponding to a radius of the polar coordinate becomes a function of the renormalization scale t and angles in the polar coordinate apart from whether it can be solved analytically. If one reaches this stage, one can implement the calculation of the RG improved effective potential in the same way as in this paper. Finally, since the stability issue and the origin of spontaneous symmetry breaking are investigated through the RG improved effective potential, our work contributes to such studies in a multiple scalar theory.

Acknowledgements

We thank T. Morozumi and Y. Shimizu for reading our manuscript and giving useful comments.

Funding

Open Access funding: SCOAP[3].

Appendix A. β and γ functions in a two real scalar model

In this appendix, we provide the β and γ functions in a two real single scalar model:

$$\begin{aligned}
\beta_{\lambda_1} &= \frac{3}{16\pi^2}(\lambda_1^2 + \lambda_3^2), \\
\beta_{\lambda_2} &= \frac{3}{16\pi^2}(\lambda_2^2 + \lambda_3^2), \\
\beta_{\lambda_3} &= \frac{\lambda_3}{16\pi^2}(\lambda_1 + \lambda_2 + 4\lambda_3), \\
\gamma_{m_1^2} &= -\frac{1}{16\pi^2 m_1^2}(\lambda_1 m_1^2 + \lambda_3 m_2^2), \\
\gamma_{m_2^2} &= -\frac{1}{16\pi^2 m_2^2}(\lambda_2 m_2^2 + \lambda_3 m_1^2), \\
\gamma_{\Lambda} &= -\frac{1}{32\pi^2 \Lambda}(m_1^4 + m_2^4) \\
\gamma_{\phi_1} &= 0, \\
\gamma_{\phi_2} &= 0.
\end{aligned}$$

References

[1] J. Elias-Miro, J. R. Espinosa, G. F. Giudice, G. Isidori, A. Riotto, and A. Strumia, Phys. Lett. B **709**, 222 (2012) [arXiv:1112.3022 [hep-ph]] [Search INSPIRE].
[2] G. Degrassi, S. Di Vita, J. Elias-Miró, J. R. Espinosa, G. F. Giudice, G. Isidori, and A. Strumia, J. High Energy Phys. **1208**, 098 (2012) [arXiv:1205.6497 [hep-ph]] [Search INSPIRE].
[3] F. Bezrukov, M. Y. Kalmykov, B. A. Kniehl, and M. Shaposhnikov, J. High Energy Phys. **1210**, 140 (2012) [arXiv:1205.2893 [hep-ph]] [Search INSPIRE].
[4] S. Alekhin, A. Djouadi, and S. Moch, Phys. Lett. B **716**, 214 (2012) [arXiv:1207.0980 [hep-ph]] [Search INSPIRE].
[5] I. Masina, Phys. Rev. D **87**, 053001 (2013) [arXiv:1209.0393 [hep-ph]] [Search INSPIRE].
[6] D. Buttazzo, G. Degrassi, P. P. Giardino, G. F. Giudice, F. Sala, A. Salvio, and A. Strumia, J. High Energy Phys. **1312**, 089 (2013) [arXiv:1307.3536 [hep-ph]] [Search INSPIRE].
[7] S. Coleman and E. Weinberg, Phys. Rev. D **7**, 1888 (1973).
[8] R. Hempfling, Phys. Lett. B **379**, 153 (1996) [arXiv:hep-ph/9604278] [Search INSPIRE].
[9] K. A. Meissner and H. Nicolai, Phys. Lett. B **648**, 312 (2007) [arXiv:hep-th/0612165] [Search INSPIRE].
[10] W.-F. Chang, J. N. Ng, and J. M. S. Wu, Phys. Rev. D **75**, 115016 (2007) [arXiv:hep-ph/0701254] [Search INSPIRE].
[11] R. Foot, A. Kobakhidze, K. L. McDonald, and R. R. Volkas, Phys. Rev. D **77**, 035006 (2008) [arXiv:0709.2750 [hep-ph]] [Search INSPIRE].
[12] S. Iso, N. Okada, and Y. Orikasa, Phys. Lett. B **676**, 81 (2009) [arXiv:0902.4050 [hep-ph]] [Search INSPIRE].
[13] M. Holthausen, M. Lindner, and M. A. Schmidt, Phys. Rev. D **82**, 055002 (2010) [arXiv:0911.0710 [hep-ph]] [Search INSPIRE].

[14] L. Alexander-Nunneley and A. Pilaftsis, J. High Energy Phys. **1009**, 021 (2010) [arXiv:1006.5916 [hep-ph]] [Search INSPIRE].
[15] K. Ishiwata, Phys. Lett. B **710**, 134 (2012) [arXiv:1112.2696 [hep-ph]] [Search INSPIRE].
[16] M. Holthausen, J. Kubo, K. S. Lim, and M. Lindner, J. High Energy Phys. **1312**, 076 (2013) [arXiv:1310.4423 [hep-ph]] [Search INSPIRE].
[17] N. Haba, H. Ishida, N. Kitazawa, and Y. Yamaguchi, Phys. Lett. B **755**, 439 (2016) [arXiv:1512.05061 [hep-ph]] [Search INSPIRE].
[18] K. Endo and Y. Sumino, J. High Energy Phys. **1505**, 030 (2015) [arXiv:1503.02819 [hep-ph]] [Search INSPIRE].
[19] B. Kastening, Phys. Lett. B **283**, 287 (1992).
[20] M. Bando, T. Kugo, N. Maekawa, and H. Nakano, Phys. Lett. B **301**, 83 (1993) [arXiv:hep-ph/9210228] [Search INSPIRE].
[21] C. Ford, D. R. T. Jones, P. W. Stephenson, and M. B. Einhorn, Nucl. Phys. B **395**, 17 (1993) [arXiv:hep-lat/9210033] [Search INSPIRE].
[22] M. B. Einhorn and D. R. Timothy Jones, Nucl. Phys. B **230**, 261 (1984).
[23] C. Ford and C. Wiesendanger, Phys. Rev. D **55**, 2202 (1997) [arXiv:hep-ph/9604392] [Search INSPIRE].
[24] C. Ford and C. Wiesendanger, Phys. Lett. B **398**, 342 (1997) [arXiv:hep-th/9612193] [Search INSPIRE].
[25] M. Bando, T. Kugo, N. Maekawa, and H. Nakano, Prog. Theor. Phys. **90**, 405 (1993) [arXiv:hep-ph/9210229] [Search INSPIRE].
[26] J. A. Casas, V. Di Clemente, and M. Quirós, Nucl. Phys. B **553**, 511 (1999) [arXiv:hep-ph/9809275] [Search INSPIRE].
[27] T. Appelquist and J. Carazzone, Phys. Rev. D **11**, 2856 (1975).
[28] T. G. Steele, Z.-W. Wang, and D. G. C. McKeon, Phys. Rev. D **90**, 105012 (2014) [arXiv:1409.3489 [hep-ph]] [Search INSPIRE].
[29] S. Iso and K. Kawana, J. High Energy Phys. **1803**, 165 (2018) [arXiv:1801.01731 [hep-ph]] [Search INSPIRE].
[30] L. Chataignier, T. Prokopec, M. G. Schmidt, and B. Świeżewska, J. High Energy Phys. **1803**, 014 (2018) [arXiv:1801.05258 [hep-ph]] [Search INSPIRE].
[31] L. Chataignier, T. Prokopec, M. G. Schmidt, and B. Świeżewska, J. High Energy Phys. **1808**, 083 (2018) [arXiv:1805.09292 [hep-ph]] [Search INSPIRE].